

A GENUINELY MULTIDISCIPLINARY JOURNAL

# CHEMPLUSCHEM

CENTERING ON CHEMISTRY

## Accepted Article

**Title:** Synthesis of Iron-oxide Palladium Nanoparticles and its catalytic applications for direct coupling of acyl chlorides with alkynes

**Authors:** Rakesh K. Sharma K Sharma; Manavi Yadav; Rashmi Gaur; Radhika Gupta; Alok Adholeya; Manoj Bhanudas Gawande

This manuscript has been accepted after peer review and the authors have elected to post their Accepted Article online prior to editing, proofing, and formal publication of the final Version of Record (VoR). This work is currently citable by using the Digital Object Identifier (DOI) given below. The VoR will be published online in Early View as soon as possible and may be different to this Accepted Article as a result of editing. Readers should obtain the VoR from the journal website shown below when it is published to ensure accuracy of information. The authors are responsible for the content of this Accepted Article.

**To be cited as:** ChemPlusChem 10.1002/cplu.201600321

**Link to VoR:** <http://dx.doi.org/10.1002/cplu.201600321>

WILEY-VCH

[www.chempluschem.org](http://www.chempluschem.org)

A Journal of



# Synthesis of Iron-oxide Palladium Nanoparticles and its catalytic applications for direct coupling of acyl chlorides with alkynes

Rakesh K. Sharma,<sup>\*[a]</sup> Manavi Yadav,<sup>[a]</sup> Rashmi Gaur,<sup>[a]</sup> Radhika Gupta,<sup>[a]</sup> Alok Adholeya<sup>[b]</sup> and Manoj B. Gawande<sup>\*[c]</sup>

**Abstract:** A new magnetic-silica based palladium nanocatalyst has been synthesized and employed for the first time in the direct coupling of acyl chlorides with terminal alkynes to prepare a variety of ynones. The synthesized nanocomposite was found to be an excellent heterogeneous catalyst for copper-free, phosphine-free, C-C bond formation through Sonogashira reaction under aerobic conditions at room temperature without the use of any additives and inert conditions. The synthesized catalyst has been comprehensively characterized by various techniques such as XRD, SEM, TEM, EDS, XPS, ICP, FT-IR, VSM, AAS, etc. This nanocatalyst can be magnetically recovered and reused up to multiple runs without any noticeable loss in its catalytic activity.

## Introduction

In current scenario, the society's driving force is to search for alternative methodologies for the formation of new bonds such as C-C, C-O, C-N, C-S, for the synthesis of a vast array of chemical compounds. Amongst all, the efficient and economical formation of carbon-carbon (C-C) bond has been the most promising reaction for the preparation of carbon scaffolds of high importance from the organic synthetic viewpoint.<sup>[1]</sup>

In recent years,  $\alpha$ ,  $\beta$ -acetylenic carbonyl derivatives, best known as ynones, have established considerable synthetic interest due to their extensive utilization as key intermediates for the synthesis of natural products, pharmaceuticals and as precursors for functional materials with interesting properties.<sup>[2]</sup> Due to their bifunctional electrophilicity and the tendency to undergo sequential nucleophilic additions and cyclizations, they have found broad application as three-carbon building blocks. They have also been extensively utilized for the synthesis of biologically active heterocyclic compounds including furans,<sup>[3]</sup> furanones,<sup>[4]</sup> isoxazoles,<sup>[5]</sup> indolizidinones,<sup>[6]</sup> pyrazoles,<sup>[7]</sup> pyrroles,<sup>[8]</sup> pyrimidines,<sup>[9]</sup> pyridinones,<sup>[10]</sup> pyridopyrimidines,<sup>[11]</sup>

and quinolines.<sup>[12]</sup>

Due to the widespread utility of ynones, considerable efforts have been devoted towards developing protocols for their synthesis using a plethora of transition metal derived catalysts. Among all, the coupling reaction of acyl chlorides and terminal alkynes catalyzed by palladium has received much attention of late due to the versatile nature of this protocol, increased functional group tolerance with improved yields and procedural simplicity.<sup>[13]</sup> However, these methods require harsh conditions such as high temperature, use of Grignard reagents, toxic phosphine ligands, unwanted side reactions, reduced yields, prolong reaction time, use of surfactants and toxic carbon dioxide.<sup>[14]</sup> In addition, the combination of Cu(I) with triethylamine has been widely employed.<sup>[15]</sup> However, use of Cu(I) catalyzed protocol involves high catalytic loading and unwanted byproducts due to homocoupling of *in-situ* generated Cu(I) acetylides. Besides suffering from various drawbacks, most of the existing methodologies utilize homogeneous catalyst, in spite of the fact that they are expensive, could not be recovered and bring about unnecessary waste and hazard to the environment.<sup>[16]</sup>

Taking these constraints into account, there is an urgent need for the design and development of efficient heterogeneous catalytic system with facile recovery from reaction media. Heterogeneous catalysts not only provide easy separation but also improve the catalytic activity and durability during the catalytic cycles by immobilizing active metal species on solid supports. Additionally, the choice of solid support plays an imperative role in catalytic activity as it is responsible in holding the active catalyst on its surface by strong co-ordination during catalysis.<sup>[17]</sup> Recent examples of such heterogeneous catalysts include ZnBr<sub>2</sub>@SiO<sub>2</sub>, Pd(II)-schiff base complex@MWCNTs, and polystyrene supported Pd(0) complex for the acylation of terminal alkynes with acyl chloride.<sup>[18]</sup> But these catalysts suffer from cumbersome filtration techniques and have little recyclability. From the sustainable perspective, high catalytic activity, easy separation and high recyclability are desirable attributes of a solid-supported metal nanocatalyst. Among various solid support materials, silica-coated magnetic nanostructures are well-recognized as they offer practical benefits over bulk supports, such as high surface area, high complex loading, excellent stability, ease of work-up, handling and separation of products, non-toxic characteristics, effortless recovery and amenability for continuous processing.<sup>[19]</sup> Besides this, the dense coating of silica not only prevents leaching of iron from the core during the catalytic activity but also assists in anchoring of other substrates. It also imparts excellent properties to magnetic nanoparticles, thereby making it inert, readily available, nontoxic and chemically stable.<sup>[20]</sup>

In continuing our efforts to develop sustainable synthetic pathways for organic transformations by using variety of advanced materials,<sup>[21]</sup> herein, we report the synthesis of a novel, highly active, palladium complex derived from a modified

[a] Rakesh K. Sharma,\* Manavi Yadav, Rashmi Gaur, Radhika Gupta  
Department of Chemistry  
University of Delhi  
105, Block-B, First floor, GCNC, University of Delhi, Delhi-110007  
E-mail: rksharmagreencem@hotmail.com

[b] Alok Adholeya  
Biotechnology and Management of Bioresources Division  
The Energy and Resources Institute  
Darbari Seth Block, IHC Complex, Lodhi Road, New delhi-110003

[c] Manoj B. Gawande\*  
Regional Centre of Advanced Technologies and materials,  
Department of Physical Chemistry, Faculty of Science,  
Palacký University, Šlechtitelů 27, 783 71, Olomouc, Czech  
Republic  
E-mail: manoj.gawande@upol.cz

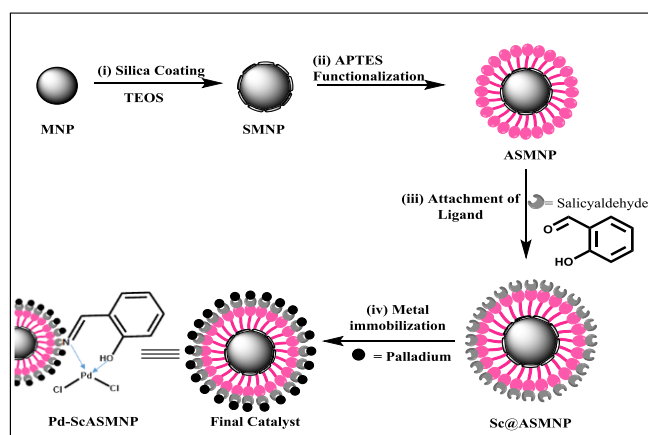
Supporting information for this article is given via a link at the end of the document. **(Please delete this text if not appropriate)**

magnetic support, capable for ynone synthesis. This nanocatalyst is of interest as it exhibits remarkable catalytic performance due to its high stability, excellent activity and effortless recovery than previously reported catalysts. Moreover, this is the first report wherein fascinating properties of silica coating and magnetic core are combined with catalytic properties of palladium for the synthesis of ynone at room temperature under copper-free and phosphine-free conditions.

## Results and Discussion

### Preparation and characterization of Pd-Sc@ASMNP

The synthesis of magnetic nanoparticles (MNPs) was performed using co-precipitation technique.<sup>[22]</sup> In order to prevent aggregation and provide stabilization to these MNPs, silica coating was performed using sol-gel approach.<sup>[23]</sup> Further, to provide scope for grafting of other substrates, the surface of magnetic silica nanoparticles (SMNPs) was covalently coupled with (3-Aminopropyl)triethoxysilane (APTES, NH<sub>2</sub> linker). APTES functionalized silica encapsulated magnetic nanoparticles (ASMNPs) were then reacted with a ligand, salicylaldehyde (Sc), and the resulting Sc@ASMNPs were metallated with palladium chloride (PdCl<sub>2</sub>) to obtain the final catalyst (Pd-Sc@ASMNPs). (Scheme 1)



**Scheme 1.** A schematic illustration of the formation of the Pd-Sc@ASMNP core-shell nano-catalyst.

For the investigation of particle size and morphology of the synthesized nanocomposites, Transmission electron microscopy (TEM) studies were conducted. Figure 1a depicts that MNPs are relatively uniform and show slight agglomeration due to absence of surfactants.<sup>[24]</sup> From the analysis of 50 colloidal aggregates of MNPs, it was found that the average size of MNPs is approximately between 8-10 nm (See the supporting information). Further, the presence of an array of bright diffraction rings in the selected area electron diffraction pattern

(Figure 1b) confirmed the crystallinity of these nanoparticles and was found to be consistent with XRD results. TEM image of SMNP in Figure 1c depicts the dark core-shell structure of MNP with almost uniform coating of silica of 4-5 nm thickness. High-resolution transmission electron microscopy (HR-TEM) image of the MNPs in Figure 1d depicts the average interplanar distance of MNPs to be ~0.20 nm, which corresponds to the (311) plane of inverse spinel structured Fe<sub>3</sub>O<sub>4</sub>.

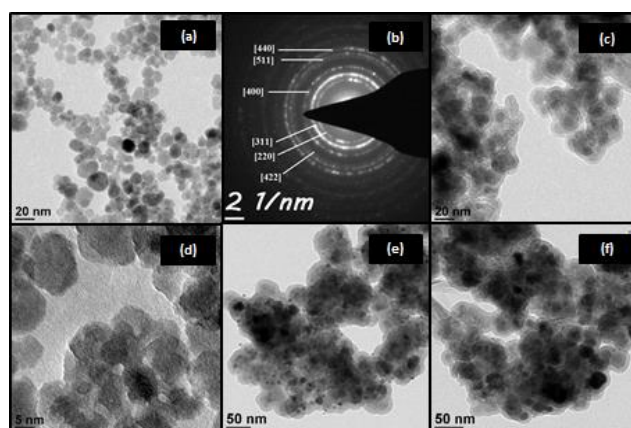


**Figure 1.** TEM images of the nanoparticles obtained at different stages of synthesis: (a) TEM image of MNPs, (b) SAED pattern of MNPs, (c) TEM image of SMNPs, (d) HR-TEM image of MNPs, (e) TEM image of fresh Pd-Sc@ASMNPs and (f) TEM image of recovered Pd-Sc@ASMNPs.

TEM image of final catalyst in Figure 1e elucidates the uniform metal binding to the core-shell surface nanocomposites. Also, the TEM image of recovered catalyst has been provided in Figure 1f to confirm that shape and morphology remain unaltered after the catalytic reaction.

Another technique that provides considerable amount of information about the topography of the sample is the Scanning electron microscopic (SEM) analysis. The transition from smooth surface of MNP to spongy surface confirms the successful coating of MNP by a silica shell. The FE-SEM images display spherical morphology of the Pd-Sc@ASMNP catalyst with slight aggregation and appears same as that of SMNP, thereby suggesting that surface modification processes did not alter the morphology of the nano-catalyst. In addition to this, the SEM image of the recovered catalyst indicates that the shape and morphology of the catalyst remain unaltered even after the reaction. (See the supporting information)

For the investigation of crystalline phase and purity of the synthesized MNP and SMNP, powder X-Ray diffraction (XRD) measurements were carried out. XRD measurement of bare MNPs in Figure 2a exhibit six characteristic Bragg peaks observed at 2 $\theta$ : 30.366°, 35.663°, 43.024°, 53.6°, 57.299°, and 62.865° which correspond to the (220), (311), (400), (422), (511) and (440) crystallographic faces of magnetite.<sup>[25a]</sup> These results were found to be consistent with the standard XRD data of the Joint Committee on Powder Diffraction Standards (JCPDS) card number (19-0629) and corresponds to inverse cubic spinel

Fe<sub>3</sub>O<sub>4</sub> crystal.<sup>[25b]</sup> The mean crystallite size of the MNPs was estimated by the Debye–Scherrer equation ( $D_{hkl} = 1/4k/\beta \cos \theta$ ), where  $D$  is the size of the axis parallel to the  $(hkl)$  plane,  $k$  is a constant with a typical value of 0.89 for spherical particles,  $\lambda$  is the wavelength of radiation,  $\beta$  is the full width at half maximum (FWHM) in radians, and  $\theta$  is the position of the diffraction peak maximum. The average crystallite size was found to be  $\sim 9.8$  nm for the (311) reflection, which is in well accordance with TEM results. In addition to the six diffraction peaks, the XRD diffraction pattern of SMNPs showed a weak broad hump at  $2\theta = 20\text{--}24^\circ$  in Figure 2b, which is the characteristic of amorphous silica.<sup>[25c]</sup> (for individual XRD peaks, see the supporting information).

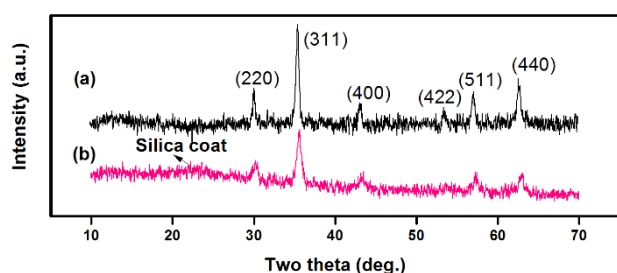


**Figure 2.** XRD pattern of the (a) MNPs and (b) SMNPs.

Energy dispersive X-ray analysis was employed to determine the composition of the synthesized nanocomposites. The EDS spectra showed well-defined peaks of palladium, silica and iron (See the supporting information), thereby confirming the successful anchoring of palladium on the nanocomposites Pd-Sc@ASMNPs. In order to quantify the amount of Pd in the final catalyst, the nanocatalyst was subjected to ICP and the corresponding metal loading was found to be  $0.08588 \text{ mmol g}^{-1}$ . Figure 3 displays the XPS spectrum of the Pd-Sc@ASMNPs. The peaks of Pd  $3d_{5/2}$  appeared at 337 eV and Pd  $3d_{3/2}$  appeared at 342 eV, confirming Pd in +2 oxidation state.<sup>[26]</sup>

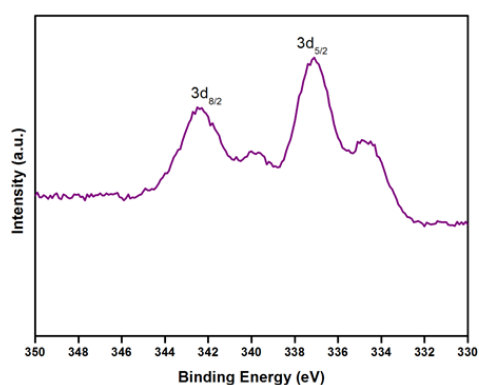


**Figure 3.** XPS spectra of Pd-Sc@ASMNPs.

Since, the presence of magnetic core inside Pd-Sc@ASMNP prevents the analysis of organic functional group by NMR spectroscopy, therefore, the FTIR technique was employed to

analyze parent nanocomposites and their further functionalization in the range of  $4000\text{--}400 \text{ cm}^{-1}$ . The IR-spectrum of MNPs depicts the Fe-O stretching absorption at  $581 \text{ cm}^{-1}$  (Figure 4a),<sup>[27a]</sup> while after silica-coating the intensity of this peak gets reduced a little (Figure 4b).<sup>[27b]</sup> Three new sharp bands appear in spectrum of SMNPs in the region of  $804$ ,  $955$  and  $1096 \text{ cm}^{-1}$ , corresponding to the Si-O-Si symmetric, Si-O symmetric and Si-O-Si asymmetric stretching modes respectively. The functionalization of APTES over SMNPs was confirmed by peaks at  $2935 \text{ cm}^{-1}$  and  $1637 \text{ cm}^{-1}$ , which are characteristic peaks for CH<sub>2</sub> and NH<sub>2</sub> from amino-propyl moiety of APTES (Figure 4c).<sup>[27c]</sup> The immobilization of ligand onto ASMNPs was indicated by the presence of C=N stretching vibration mode at  $1652 \text{ cm}^{-1}$  (Figure 4d) and its further metallation with PdCl<sub>2</sub> was observed by the shift of the prominent peak  $1652 \text{ cm}^{-1}$  to  $1644 \text{ cm}^{-1}$  indicating strong metal-ligand interaction (Figure 4e).<sup>[27d, 27e]</sup> (for detailed IR spectra, see the supporting information).

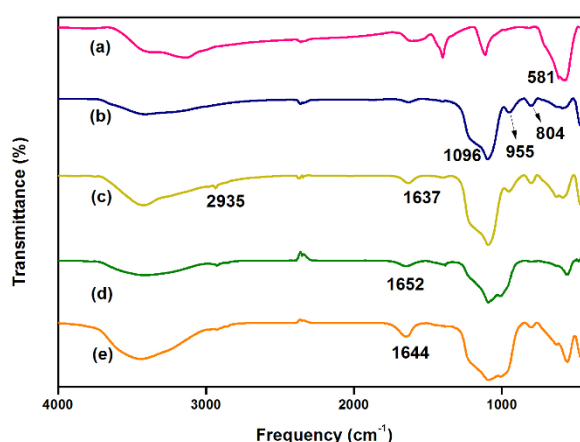


**Figure 4.** FT-IR spectra of (a) MNPs, (b) SMNPs, (c) ASMNPs, (d) Sc@ASMNPs, and (e) Pd-Sc@ASMNPs.

The field-dependent magnetization measurements of synthesized nanocomposites were conducted. The Figure 5 displays magnetization curves which display no hysteresis indicating that the nanoparticles exhibit superparamagnetic behavior at room temperature. Besides this, the superparamagnetic behavior was also confirmed by the inset in Figure 5 which shows negligible coercivity and remanence in the absence of an external applied magnetic field. The saturation magnetization value of MNPs was found to be  $56 \text{ emu/g}$ , which is lower than its bulk counterpart ( $90 \text{ emu/g}$ ), indicating that particle size affects the magnetization value of the particle under applied field.<sup>[28]</sup> In addition, functionalization of MNPs resulted in further reduction of the magnetization value which can be accredited to the contribution made by non-magnetic silica shell and other functional groups present at the surface of magnetic core. The magnetization value came out to be  $41 \text{ emu/g}$  for SMNPs,  $27 \text{ emu/g}$  for ASMNPs and  $19 \text{ emu/g}$  for final nanocatalyst Pd-Sc@ASMNPs. In spite of exhibiting lower magnetization value, the net magnetism of final nanocatalyst was sufficiently high for its effective separation from the reaction mixture *via* external magnet.

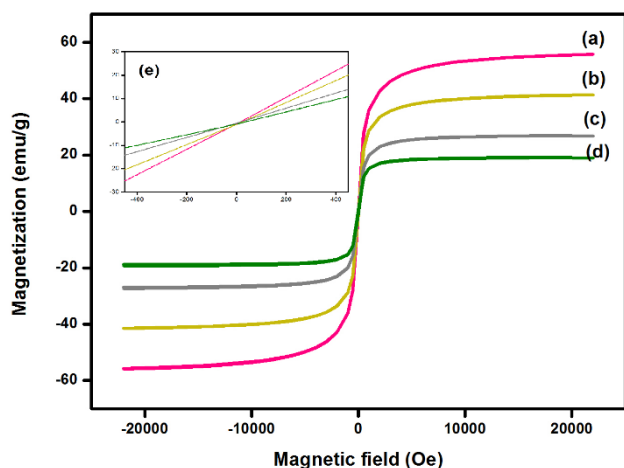


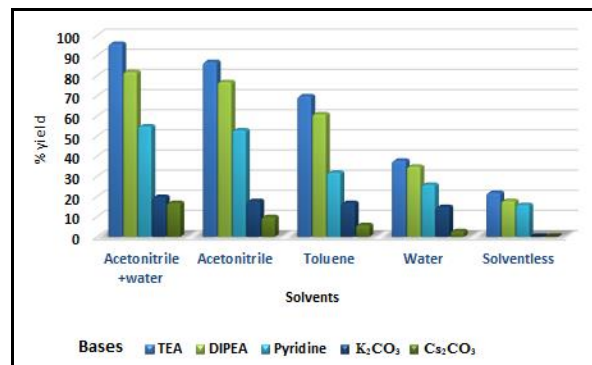
**Figure 5.** Magnetization curves obtained by VSM at room temperature for (a) MNPs, (b) SMNPs, (c) ASMNPs, (d) Pd-Sc@ASMNPs and (e) inset: enlarged image near the coercive field.

#### Catalytic activity of Pd-Sc@ASMPs for direct coupling of acyl chlorides with terminal alkynes

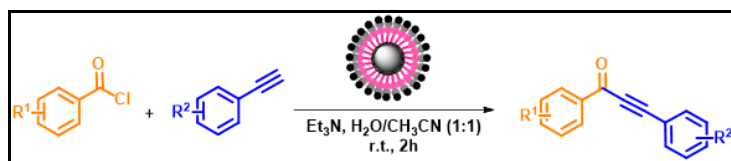
In order to test the efficacy of the prepared nanocatalyst Pd-Sc@ASMNPs and to determine the optimal reaction conditions, benzoyl chloride and phenylacetylene were selected as the prototype. As a starting point to optimize the Sonogashira coupling reaction, the impact of different reaction parameters such as solvents, base and catalyst amount was evaluated under aerobic conditions. As can be seen from Figure 6, among various base and solvent combinations, highest yield was obtained when triethylamine was used as base and 1:1 ratio of acetonitrile and water was used as solvent. We also found that the higher reaction temperatures did not favour the cross-coupling reaction. Consequently, all the reactions were performed at room temperature. For the determination of the optimal catalytic amount, we conducted a blank test, where no significant yield was obtained. While the reaction gave product when 10 mg of catalyst was employed, but further enhancement in the yield of product was observed when 20 mg of catalyst was taken. However, no further increase in the yield was observed with 30 mg of catalyst. Therefore, the best results were obtained with 20 mg of catalyst (See the supporting information).

To examine the scope of this coupling reaction, various acid chlorides (aliphatic, aromatic and heteroaromatic) were coupled with terminal alkynes using the optimized methodology (Table 1). It was observed that the reaction gave good yields in 2 hours demonstrating the effectiveness of the catalytic system. To further expand the generality of this coupling reaction, we investigated a variety of aroyl chlorides having both activating and deactivating groups such as methyl, methoxy, chloro, and nitro. It was observed that the reaction was equally facile for both electron donating and electron withdrawing substituents on the aroyl chlorides. However, electron withdrawing substituents such as  $\text{NO}_2$ , took longer to form coupling products, although high conversions were still obtained (Table 1, entries 5, 13). Besides, the nature and the position of substitution in the aromatic ring did not have much effect on the reaction (Table 1, entries 2, 3, 15, 16). Also,

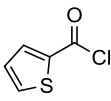
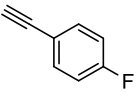
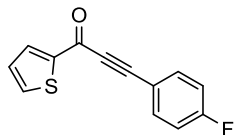
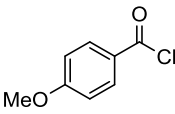
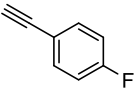
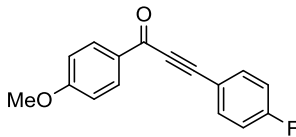
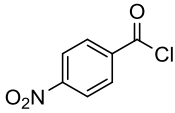
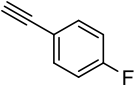
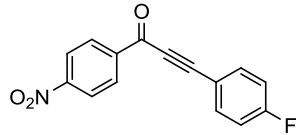
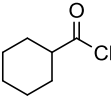
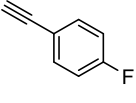
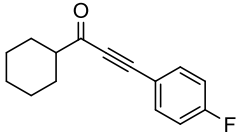
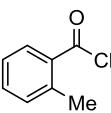
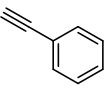
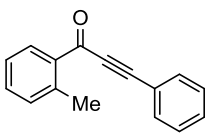
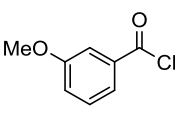
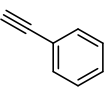
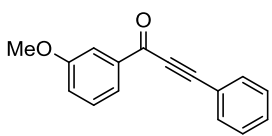
heteroaryl acid chloride such as 2-thiophene carbonyl chloride reacted smoothly with terminal alkynes to give the corresponding ynones in excellent yields (Table 1, entries 6, 11). Under the same reaction conditions, cyclohexane carbonyl chloride also afforded the desired coupling products in good yields (Table 1, entries 7, 14).



**Figure 6.** Effect of base and solvent on acylation of terminal alkynes (Reaction conditions: Benzoyl chloride (1.0 mmol); Phenyl acetylene (1.2 mmol); Pd-Sc@ASMNPs (20 mg); room temperature; 2 h).

**Table 1.** Scope of catalytic activity of the Pd-Sc@ASMNPs in synthesis of ynones<sup>a</sup>

Entry	Aroyl chloride	Acetylene	Product	Yield (%) <sup>b</sup>	TON <sup>c</sup>
1				96	559
2				95	553
3				96	559
4				94	547
5 <sup>d</sup>				89	518
6				97	565
7				90	524
8				91	529
9				90	524
10				92	536

11				94	547
12				93	542
13 <sup>d</sup>				83	483
14				85	495
15				95	553
16				95	553

<sup>a</sup>Reaction conditions: Aroyl chloride (1.0 mmol); Acetylene (1.2 mmol); Catalyst (20 mg); Et<sub>3</sub>N (1.5 eq); 2 mL of acetonitrile and water mixture (1:1); Room temperature; Time 2 h.

<sup>b</sup>yields were determined by GC-MS.

<sup>c</sup>TON= Calculated using the 0.0017 mmol/g palladium (Obtained by ICP for 20 mg of Pd-Sc@ASMNPs). <sup>d</sup>reaction time 3 h.

Finally, in order to show the merit of this catalytic method, we compared our obtained results with the previously reported work (see the supporting information), and found that our catalyst worked much more efficiently without additives. Hence, catalytic efficiency of the present catalytic system is remarkable in terms of mild reaction conditions, short reaction time and easy recovery of the catalyst.

The reusability of the catalyst was also examined. After each experiment, the catalyst was separated from the reaction mixture by using external magnet, washed with ethyl acetate and ethanol and dried under vacuum before its use in subsequent reactions. After being recovered, the catalyst was used up to six runs without noticeable deactivation (Figure 7). SEM and TEM images of the recovered catalysts further provided evidence of unaltered structure and morphology (Figure 1f, and S2d), while EDS confirmed the presence of palladium in the recovered catalyst (See the supporting information).

#### Hot-filtration Test

Estimation of the leaching rate and the heterogeneity nature of the catalyst was determined by performing two corresponding

set of experiments. In the first set, standard reaction was performed and after the completion of the reaction, the catalyst was separated using external magnet and the filtrate was analysed under AAS, which showed negligible leaching. In the second set, split test was conducted, where, a standard reaction was carried out with catalyst for half an hour, which corresponds to approximately 20-25% of the conversion by GC-MS. Then, the nanocatalyst was removed from the reaction mixture using magnet and the reaction was continued further. It was observed that, no coupling product was detected up to 3 hours in the reaction mixture under the same conditions, thereby indicating truly heterogeneous nature of the magnetic nanocatalyst.



**Figure 7.** Catalyst recycling test for six consecutive runs in the synthesis of ynones.

### Proposed catalytic mechanism

With regard to the mechanistic path for the present transformation, the plausible mechanism would be the formation of Pd(0) species (C) from the precursor (A) *via* intermediate (B) and homocoupling of terminal alkynes. This is followed by the oxidative addition of acid chloride to form intermediate (D). Subsequent alkyne coordination results in the formation of acyl palladium complex (F) *via* intermediate (E). In the final step, the product is obtained in reductive elimination along with the regeneration of the catalyst<sup>[18e,29]</sup> (Figure 8).

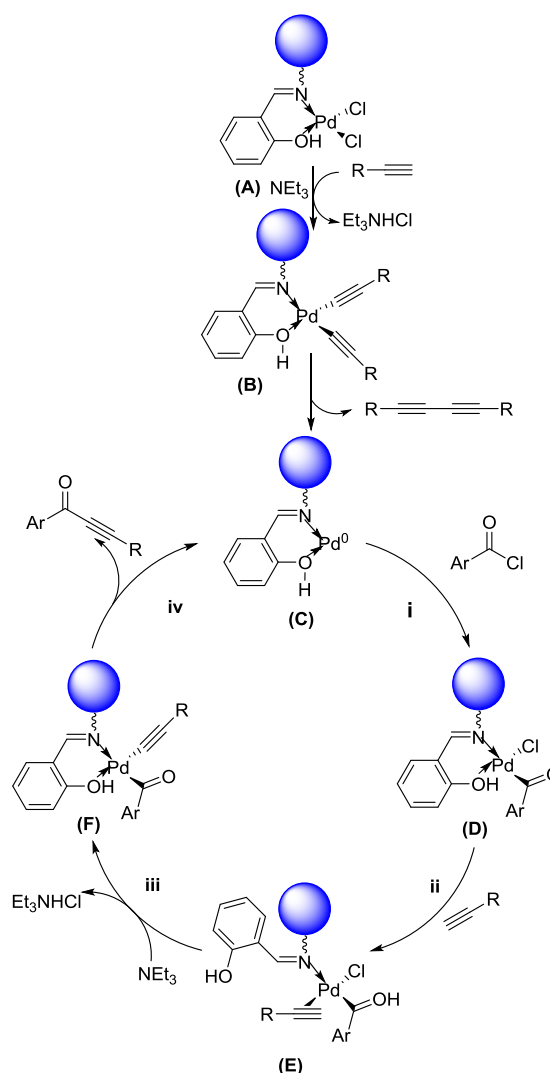


**Figure 8.** Proposed reaction mechanism.

### Conclusions

In summary, the Pd-Sc@ASMNPs nanocatalyst was fabricated successfully *via* a facile route. These nanocomposites endowed large surface area, good durability, and excellent catalytic activity towards the synthesis of ynones *via* Sonogashira cross-coupling reaction with excellent yields and high turn-over number. These methodologies provide a facile, efficient and sustainable process for the C-C coupling and have wide applicability towards a variety of acyl chlorides under mild conditions. Moreover, the effortless recovery and reusability of the catalyst for at least six runs without any marked loss of activity makes it an efficient protocol to yield combinatorial libraries of ynones. The reported outcomes open up the possibility of using Pd-Sc@ASMNPs nanocatalyst for other organic transformations and large scale industrial applications.

## Experimental Section

### General remarks

TEOS and APTES were obtained from Sigma-Aldrich and Fluka respectively. Ferric sulphate and ferrous sulphate were purchased from Sisco Research Laboratory. All the other reagents used were of analytical grade and obtained from Spectrochem and Merck. Double distilled water was used throughout the studies.

### Characterization

Powder X-ray diffraction (XRD) patterns were performed using a Bruker D8 Advance diffractometer (Karlsruhe, bundesland, Germany) in the 2 $\theta$  range of 10–80°. FT-IR spectra were recorded on Perkin-Elmer Spectrum 2000 using KBr pellets. TEM images were acquired using FEI TECHNAI G2 T20 transmission electron microscope operated at 200 kV with an energy dispersive X-ray analyser. ImageJ software was used for image processing and analysis. SEM images were obtained from Carl Zeiss India scanning electron microscope. Digestions were performed on Anton Paar multiwave 3000. The Pd content was determined using Inductively coupled Plasma of PerkinElmer Optima 2100 DV and LABINDIA AA 7000 Atomic Absorption Spectrometer with acetylene flame. The XPS spectrum was recorded on Omicron Make XPS system interface with EA 125 Energy Analyzer within monochromatic Aluminium K $\alpha$  X-Ray source with energy of 1486.6 eV with energy resolution of 0.6 eV. The magnetization values were obtained from vibrating sample magnetometer (EV-9, Microsense, ADE). The derived products were analyzed and confirmed on GC-MS (Agilent gas Chromatography, 6850 GC with a HP-5MS) and a quadrapole mass filter equipped 5975 mass selective detector (MSD) using helium as carrier gas. BET study was performed on Quantachrome Instruments Model: ASI-CI-11 Adsorbate temperature 77 K, found that the surface area of final nano-catalyst Pd-Sc@ASMNPs is 113 m<sup>2</sup>/g. NMR spectra were recorded on a 400 MHz JEOL NMR spectrometer in deuterated chloroform (CDCl<sub>3</sub>).

### Synthesis of Magnetic Nanoparticles (MNPs)

MNPs were synthesized using co-precipitation method where, both ferric (6.0 g) and ferrous sulphate (4.2 g) were dissolved in water (250 mL) under stirring at 60 °C resulting in a yellowish-orange solution. To this, 25% NH<sub>4</sub>OH (15 mL) was added with vigorous mechanical stirring resulting in black precipitates. Then, the stirring was continued till half an hour. The precipitated MNPs were separated using magnet and washed several times with deionized water and ethanol.

### Synthesis of silica-coated MNPs (SMNPs)

Silica coating of these MNPs was performed via sol-gel approach where, a suspension of MNPs and 0.1 M HCl (2.2 mL) in ethanol and water (50 mL) was kept under sonication. To this, 5 mL of 25% NH<sub>4</sub>OH was added followed by 1 mL TEOS addition and was kept for stirring at 60 °C for six hours. The obtained materials were then separated magnetically and washed with ethanol and dried under vacuum.

### Synthesis of APTES functionalized SMNPs (ASMNPs)

For the incorporation of amine groups onto surface of SMNPs, APTES (0.5 mL) was added to disperse solution of 0.1 g of SMNPs in 100 mL of ethanol and the resulting solution was stirred at 50 °C for 6 h. The APTES functionalized SMNPs were separated with magnet and washed several times with ethanol to remove the unreacted silylating agent.

### Synthesis of the final catalyst Pd-Sc@ASMNPs

For covalent grafting of the ligand on ASMNPs, 1 g of ASMNP was refluxed with 2 mmol of salicylaldehyde (Sc) in acetone (100 mL) along with molecular sieves for 3 h. The obtained product was washed with ethanol and dried under vacuum. Finally, 0.5 g of grafted Sc@ASMNPs was stirred with a solution of 0.1 mmol of PdCl<sub>2</sub> in acetone for 3 h. The resulting Pd-Sc@ASMNPs were separated magnetically and thoroughly washed with deionized water and dried under vacuum.

### General procedure for Pd-Sc@ASMNPs nanocatalyst mediated synthesis of ynones

For this purpose, 10 mL of round bottom flask was charged with benzoyl chloride (1.0 mmol), 1:1 ratio of acetonitrile and water (2 mL) and triethylamine (1.5 eq). To this, 1.2 mmol of terminal alkyne was added along with the catalyst (20 mg) and the reaction was kept under room temperature and aerobic conditions till its completion. The reaction was monitored using thin layer chromatography and aliquots were analysed on regular intervals using GC-MS. Finally, all the products were extracted by ethyl acetate, dried over sodium sulphate, concentrated and were confirmed by GC-MS (See SI).

### Recycling procedure

After the reaction completion, the catalyst was separated using an external magnet followed by washing with ethyl acetate and ethanol. Then, the catalyst was used directly for next consecutive runs without further purification.

## Acknowledgements

One of the authors, Manavi Yadav thanks TERI, Gwal Pahari, Gurgaon and USIC, University of Delhi, Delhi for providing instrumental facilities. The authors acknowledge the assistance provided by the Research Infrastructure NanoEnvicZ, supported by the Ministry of Education, Youth and Sports of the Czech Republic under Project No. LM2015073, and support from the Ministry of Education, Youth and Sports of the Czech Republic – project No. LO1305.

**Keywords:** Palladium based • Silica-coated magnetic nanocatalysts • Sonogashira coupling • Synthesis of ynones •

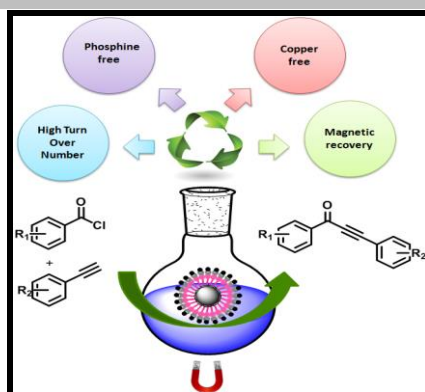
- [1] (a) X, -F. Wu, H. Neumann and M. Beller, *Chem. Soc. Rev.*, 2011, **40**, 4986–5009; (b) H. -Y. Jang and M. J. Krische, *Acc. Chem. Res.*, 2004, **37**, 653–661; (c) V. Ritleng, C. Sirlin, and M. Pfeffer, *Chem. Rev.*, 2002, **102**, 1731–1769; (d) A. H. Cherney, N. T. Kadunce, and S. E. Reisman, *Chem. Rev.*, 2015, **115**, 9587–9652; (e) C. -J. Li, *Chem. Rev.*, 2005, **105**, 3095–3165.
- [2] (a) J. M.-Contelles, E. de Opazo, *J. Org. Chem.*, 2002, **67**, 3705–3717; (b) C. J. Forsyth, J. Xu, S. T. Nguyen, I. A. Samdal, L. R. Briggs, T. Rundberget, M. Sandvik, C. O. Miles, *J. Am. Chem. Soc.*, 2006, **128**, 15114–15116; (c) A. Arcadi, M. Aschi, F. Marinelli, M. Verdecchia, *Tetrahedron* 2008, **64**, 5354–5361; (d) C.A. Quesnelle, P. Gill, M. Dodier, D. St-Laurent, M. Serrano-Wu, A. Marinier, A. Martel, C.E. Mazzucco, T.M. Sticle, J.F. Barrett, D.M. Vyas and B.N. Balasubramanian, *Bioorg. Med. Chem. Lett.*, 2003, **13**, 519–524.

- [3] (a) A. Jeevanandam, K. Narkunan and Y.-C. Ling, *J. Org. Chem.*, 2001, **66**, 6014-6020; (b) A. V. Kel'in and V. Gevorgyan, *J. Org. Chem.*, 2002, **67**, 95-98.
- [4] (a) H. Arzumaniyan, M. Jean, D. Nuel, A. Cabrera, J. L. G. Gutierrez and N. Rosas, *Organometallics*, 1995, **14**, 5438-5441; (b) B. G. Van denHoven, B. El Ali and H. Alper, *J. Org. Chem.*, 2000, **65**, 4131-4137; (c) V. Lellek and H. -J. Hansen, *Helv. Chim. Acta*, 2001, **84**, 3548-3580.
- [5] M. Hojo, K. Tomita and A. Hosomi, *Tetrahedron Lett.*, 1993, **34**, 485-488.
- [6] R. K. Dieter and K. Lu, *J. Org. Chem.*, 2002, **67**, 847-855.
- [7] (a) D. B. Grotjahn, S. Van, D. Combs, D. A. Lev, C. Schneider, M. Rideout, C. Meyer, G. Hernandez and L. Mejorado, *J. Org. Chem.*, 2002, **67**, 9200-9209; (b) X. Wang, J. Tan and L. Zhang, *Org. Lett.*, 2000, **2**, 3107-3109.
- [8] A. V. Kel'in, A. W. Sromek and V. Gevorgyan, *J. Am. Chem. Soc.*, 2001, **123**, 2074-2075.
- [9] (a) A. S. Karpov and T. J. J. Muller, *Org. Lett.*, 2003, **5**, 3451-3454; (b) M. C. Bagley, D. D. Hughes and P. H. Taylor, *Synlett*, 2003, 259-261.
- [10] C. G. Savarin, J. A. Murry and P. G. Dormer, *Org. Lett.*, 2002, **4**, 2071-2074.
- [11] (a) M. C. Bagley, D. D. Hughes, R. Lloyd and V. E. C. Powers, *Tetrahedron Lett.*, 2001, **42**, 6585-6588; (b) D. D. Hughes and M. C. Bagley, *Synlett*, 2002, 1332-1334.
- [12] A. Arcadi, F. Marinelli and E. Rossi, *Tetrahedron*, 1999, **55**, 13233-13250.
- [13] (a) R. Chinchilla and C. Najera, *Chem. Rev.*, 2014, **114**, 1783-1836; (b) E. Negishi, V. Bagheri, S. Chatterjee, F. T. Luo, J. A. Miller and A. T. Stoll, *Tetrahedron Lett.*, 1983, **24**, 5181-5184; (c) *Handbook of Organopalladium Chemistry for Organic Synthesis*; Negishi, E.-I., de Meijere, A., Eds.; John Wiley & Sons: New York, 2002; (d) M. S. Mohamed Ahmed and A. Mori, *Org. Lett.*, 2003, **5**, 3057-3060.
- [14] (a) Y. Tohda, K. Sonogashira and N. Hagihara, *Synthesis*, 1977, 777-778; (b) D. A. Alonso, C. Najera and M. C. Pacheco, *J. Org. Chem.*, 2004, **69**, 1615-1619; (c) L. Chen and C. J. Li, *Org. Lett.*, 2004, **6**, 3151-3153; (d) R. J. Cox, D. J. Ritson, T. A. Dane, J. Berge, J. P. H. Charmant and A. Kantacha, *Chem. Commun.*, 2005, **8**, 1037-1039.
- [15] (a) E. Mohammadi, B. Movassagh and M. Navidi, *Helv. Chim. Acta.*, 2014, **97**, 70-75; (b) W. Sun, Y. Wang, X. Wu and X. Yao, *Green Chem.*, 2013, **15**, 2356-2360; (c) W. Yin, H. He, Y. Zhang, D. Luo and H. He, *Synthesis*, 2014, **46**, 2617-2621.
- [16] (a) H. Yuan, Y. Shen, S. Yu, L. Shan, Q. Sun and W. Zhang, *Synth. Commun.*, 2013, **43**, 2817-2823; (b) D. A. Alonso, C. Najera and M. C. Pacheco, *J. Org. Chem.*, 2004, **69**, 1615-1619; (c) S. S. Palimkar, P. H. Kumar, N. R. Jogdand, T. Daniel, R. J. Lahoti and K. V. Srinivasan, *Tetrahedron Lett.*, 2006, **47**, 5527-5530; (d) C. Taylor and Y. Bolshan, *Org. Lett.*, 2014, **16**, 488-491.
- [17] (a) R. Hudson, Y. Feng, R. S. Varma and A. Moores, *Green Chem.*, 2014, **16**, 4493-4505; (b) R. B. N. Baig and R. S. Varma, *Chem. Commun.*, 2013, **49**, 752-770; (c) M. B. Gawande, P. S. Branco and R. S. Varma, *Chem. Soc. Rev.*, 2013, **42**, 3371-3393; (d) V. Polshettiwar and R. S. Varma *Green Chem.*, 2010, **12**, 743-754.
- [18] (a) A. Keivanloo, M. Bakherad, B. Bahramian and S. Baratnia, *Tetrahedron Lett.*, 2011, **52**, 1498-1502; (b) M. Navidi, B. Movassagh and S. Rayati, *Appl. Catal. A*, 2013, **452**, 24-28; (c) M. Bakherad, A. Keivanloo, B. Bahramian and S. Jajarmi, *Synlett*, 2011, **3**, 311-314; (d) M. Genelot, V. Dufaud and L. Djakovitch, *Adv. Synth. Catal.*, 2013, **355**, 2604-2616; (e) S. Santra, K. Dhara, P. Ranjan, P. Bera, J. Dash and S. K. Mandal, *Green Chem.*, 2011, **13**, 3238-3247; (f) M. A. Bhosale, T. Sasakib and B. M. Bhanage, *Catal. Sci. Technol.*, 2014, **4**, 4274-4280.
- [19] (a) M. B. Gawande, Y. Monga, R. Zboril, R. K. Sharma, *Coord. Chem. Rev.*, 2015, **288**, 118-143; (b) S. Zhou, M. Johnsona and J. G. C. Veinot, *Chem. Commun.*, 2010, **46**, 2411-2413; (c) G. A. Sotiriou, A. M. Hirt, P. Y. Lozach, A. Teleki, F. Krumeich and S. E. Pratsinis, *Chem. Mater.*, 2011, **23**, 1985-1992; (d) Y. Lien and T. M. Wu, *J. Colloid Interface Sci.*, 2008, **326**, 517-521; (e) Y. Lu, Y. Yin, B. T. Mayers and Y. Xia, *Nano Lett.*, 2002, **2**, 183-186; (f) S. Kralj, M. Drogenik and D. Makovec, *J. Nanopart. Res.*, 2011, **13**, 2829-2841.
- [20] (a) R. K. Sharma, S. Sharma, S. Dutta, R. Zboril 30 and M. B. Gawande, *Green Chem.*, 2015, **17**, 3207-3230; (b) S. C. Tsang, C. H. Yu, X. Gao and K. Tam, *J. Phys. Chem. B*, 2006, **110**, 16914-16922; (c) D. Niu, Y. Li, X. Qiao, L. Li, W. Zhao, H. Chen, Q. Zhao, Z. Mac and J. Shi, *Chem. Commun.*, 2008, **37**, 4463-4465; (d) J. L. V. Escoto, R. C. H. Phillips and W. Lin, *Chem. Soc. Rev.*, 2012, **41**, 2673-2685.
- [21] (a) M.B. Gawande, A. Rathi, I.D. Nogueira, R.S. Varma, P.P. Branco, *Green Chem.*, 2013, **15**, 1895-1899; (b) M.B. Gawande, P.S. Branco, R.S. Varma, *Chem. Soc. Rev.* 2013, **42**, 3371-3393.; (c) R. K. Sharma, Y. Monga, A. Puri and G. Gaba, *Green Chem.*, 2013, **15**, 2800-2809; (d) M.B. Gawande, S.N. Shelke, R. Zboril, R.S. Varma, *Acc. Chem. Res.* 2014, **47**, 1338-1348.; (e) R. K. Sharma, M. Yadav, R. Gaur, Y. Monga and A. Adholeya, *Catal. Sci. Technol.*, 2015, **5**, 2728-2740; (f) R. K. Sharma, M. Yadav, Y. Monga, R. Gaur, A. Adholeya, R. Zboril, R. S. Varma and M. B. Gawande, *ACS Sustainable Chem. Eng.*, 2016, DOI: 10.1021/acssuschemeng.5b01183; (g) R. K. Sharma, R. Gaur, M. Yadav, A. K. Rathi, J. Pechousek, M. Petr, R. Zboril, and M. B. Gawande, *ChemCatChem*, 2015, **7**, 3495 - 3502.
- [22] V. Polshettiwar, R.S. Varma, *Org. Biomol. Chem.*, 2009, **7**, 37-40.
- [23] Z. Zhang, F. Zhang, Q. Zhu, W. Zhao, B. Ma and Y. Ding, *J. Colloid Interface Sci.*, 2011, **360**, 189-194.
- [24] (a) S. Wang, Z. Zhang, B. Li and J. Li, *Catal. Sci. Technol.*, 2013, **3**, 2104-2112; (b) J. Wang, S. Zheng, Y. Shao, J. Liu, Z. Xu and D. Zhu, *J. Colloid Interface Sci.*, 2010, **349**, 293-299.
- [25] (a) R. A. -Reziq and H. Alper, *Appl. Sci.*, 2012, **2**, 260-276; (b) R. A. -Reziq, H. Alper, D. S. Wang and M. L. Post, *J. Am. Chem. Soc.*, 2006, **128**, 5279-5282; (c) Q. Zhang, H. Su, J. Luo and Y. Wei, *Green Chem.*, 2012, **14**, 201-208.
- [26] G. Kumar, J. R Blackburn, R. G. Albrtdge, W. E. Moddeman, and M. M. Jones, *Inorg. Chem.*, 1972, **2**, 296-300.
- [27] (a) J. Zhu, J. He, X. Du, R. Lu, L. Huang and X. Ge, *Appl. Surf. Sci.*, 2011, **257**, 9056-9062; (b) M. Kooti and M. Afshari, *Mater. Res. Bull.*, 2012, **47**, 3473-3478; (c) M. Yamaura, R. L. Camilo, L. C. Sampaio, M. A. Macedo, M. Nakamurad and H. E. Toma, *J. Magn. Magn. Mater.*, 2004, **279**, 210-217; (d) M. M. Farahani and N. Tayyebi, *J. Mol. Catal. A: Chem.*, 2011, **348**, 83-87; (e) M. Esmailpour, A. R. Sardariana, and J. Javidi, *Appl. Catal., A*, 2012, **445-446**, 359-367.
- [28] (a) A. Hu, G. T. Yes and W. Lin, *J. Am. Chem. Soc.*, 2005, **127**, 12486-12487; (b) R. G. Digigowa, J.-F. Dechezelles, H. Dietsch, I. Geissbühler, D. Vanhecke, C. Geers, A.M. Hirt, B. R. Rutishauser and A. P. Fink, *J. Magn. Magn. Mater.*, 2014, **362**, 72-79.
- [29] (a) H. Plenio, *Angew. Chem. Int. Ed.*, 2008, **47**, 6954 -6956; (b) A. Tougerti, S. Negri, and A. Jutand, *Chem. Eur. J.*, 2007, **13**, 666 - 676; (c) H. Lu, L. Wang, F. Yang, R. Wua and W. Shen, *RSC Adv.*, 2014, **4**, 30447-30452.

## The Table of Contents

## FULL PAPER

A new magnetic-silica based palladium nanocatalyst synthesized and applied for the first time in the direct coupling of acyl chlorides with terminal alkynes to prepare a variety of ynones under copper-free, phosphine-free, and aerobic conditions at room temperature without the use of any additives and inert conditions.



Rakesh K. Sharma,<sup>\*a</sup> Manavi Yadav,<sup>a</sup>  
Rashmi Gaur,<sup>a</sup> Radhika Gupta,<sup>a</sup> Alok  
Adholeya<sup>b</sup> and Manoj B. Gawande<sup>\*c</sup>

Page No. – Page No.

**Silica-based Magnetite core-shell  
Palladium Nano-catalyst in the  
synthesis of ynones under copper-  
free and phosphine-free conditions**